ADVANCED SENSOR RESEARCH Open Access
www.advsensorres.com

Exploring Gelatin-A and Mouse Proline-Rich Protein 5 as Probes for Wine Polyphenol Analysis by Quartz Crystal Microbalance with Dissipation Monitoring

*Giorgia Tori, Mariacristina Gagliardi, Francesco Lunardelli, Chiara Sanmartin, Isabella Taglieri, Gianmarco Alfieri, Margherita Modesti, Domenica Convertino, Andrea Bellincontro, Fabio Mencarelli, and Marco Cecchini**

Polyphenols are significant compounds that impact the winemaking process, influencing key attributes such as wine quality, color, astringency, bitterness, and chemical stability. Traditionally, the wine polyphenolic content is assessed through conventional analytical methods, which are costly and time-consuming. Thus, developing novel strategies to overcome these limitations is highly desirable. Quartz Crystal Microbalance with Dissipation Monitoring (QCM-D) is an electromechanical sensor that has gained broad recognition as a fast, reliable, and label-free detection tool. The QCM-D is employed to investigate Gelatin Type A (Gel-A) and Mouse Proline-Rich Protein 5 (MP5) as probes for analyzing polyphenols in red wines. The probes have been successfully immobilized on the sensor surface, yielding molecular densities of 2.1×10^{14} and 5.1×10^{12} molecules cm^{-2} for MP5 and Gel-A, respectively. Both probes have shown promising performance in the analysis of polyphenols in wine, with both changes in the sensor's resonance frequency and dissipation with all tested samples. Notably, using MP5, a linear response of the dissipation has been observed with both the total polyphenol and hydroxybenzoic acid concentrations. These results indicate strong potential for developing a stand-alone sensor platform to directly monitor polyphenols during the winemaking process.

1. Introduction

Polyphenols are secondary metabolites synthesized by all higher plants, playing a crucial role in responding to both biotic factors, such as plant pathogens and herbivore aggressions, and abiotic stressors, including UV-rays.[1]

Polyphenols, present in the solid parts of grapes (such as skin, pulp, and seeds), are also essential in winemaking as they significantly influence the quality of wine. While pulp is the primary source of polyphenols for white and rosé wines, red wines derive them from all parts of the grape (including skin and seeds).[2] Polyphenols also affect the organoleptic properties of wine, with specific subclasses contributing to distinct features. For instance, anthocyanins, along with hydroxybenzoic and hydroxycinnamic acids, are responsible for the color of wine. Additionally, condensed tannins contribute to the astringency and bitterness of wine.[3]

G. Tori, M. Gagliardi, F. Lunardelli, M. Cecchini
NEST
Istituto Nanoscienze-CNR and Scuola Normale Superiore
Piazza San Silvestro, Pisa I-56127, Italy
E-mail: marco-cecchini@cnr.it

C. Sanmartin, I. Taglieri, F. Mencarelli
University of Pisa
Department of Agriculture Food Environment
University of Pisa
Via Del Borghetto 80, Pisa I-56124, Italy

C. Sanmartin, I. Taglieri
Interdepartmental Research Center
Nutraceuticals and Food for Health
University of Pisa
Via Del Borghetto 80, Pisa I-56124, Italy

G. Alfieri, M. Modesti, A. Bellincontro
Department for Innovation of Biological
Agrofood and Forest Systems (DIBAF)
University of Tuscia
Via De Lellis, Viterbo 01100, Italy

D. Convertino
Center for Nanotechnology Innovation @NEST
Istituto Italiano di Tecnologia
Piazza San Silvestro 12, Pisa 56127, Italy

The ORCID identification number(s) for the author(s) of this article can be found under https://doi.org/10.1002/adsr.202400140

DOI: 10.1002/adsr.202400140

Currently, the gold standard techniques to evaluate the global polyphenolic content of wine include spectrophotometric and chromatographic methods. A commonly used spectrophotometric method for phenolic quantification is based on measuring the absorption at 280 nm, which corresponds to the characteristic absorption of benzene rings present in most phenolic compounds.[4] However, this approach has some limitations. For example, cinnamic acids and chalcones do not exhibit maximum absorption at this wavelength. Additionally, non-phenolic molecules, such as certain amino acids, also contain benzene rings and may absorb at 280 nm, potentially causing interference with the measurements. Another frequently employed method is the Folin-Ciocalteu assay, which relies on the reductive properties of phenols to quantify their concentration. In this assay, phenolic compounds reduce phosphomolybdic acid, resulting in a blue-colored complex under alkaline conditions. However, its specificity is limited, as other reducing agents, such as ascorbic acid, and phenolic groups found in proteins may also participate in the reaction, leading to non-specific results.[4]

In addition to the methods previously mentioned, High-Performance Liquid Chromatography (HPLC) is commonly used for the separation and quantification of polyphenols, often coupled with detection techniques such as UV spectroscopy.[4] However, there are some limitations to its use in enology. For instance, when analyzing wine, sample preparation is often necessary to simplify the complexity of the chromatograms. Moreover, HPLC is a time-consuming and costly technique, which can make it less suitable for routine analysis in this context.[5] Due to these challenges, the wine industry is currently exploring alternative approaches to overcome these limitations.

Various strategies for detecting polyphenols in wine are documented in the literature, including amperometric biosensors[6–13], cyclic voltammetry-based,[14,15] colorimetric[16], and spectrophotometric[17] sensors. While all these approaches are undeniably intriguing and attractive alternatives to the conventional methods, they often involve sample preparation steps, such as solid-phase extraction or wine dilution. Furthermore, the aforementioned amperometric biosensors rely on the use of enzymes as biorecognition elements, which can present several drawbacks, including broad substrate specificity, potential inactivation of enzymatic functional groups during immobilization, and limited stability of catalytic activity over time.[18–20]

Cyclic voltammetry also has some limitations related to the presence of other antioxidant compounds in wine, such as sulfur dioxide and ascorbic acid, in addition to polyphenols, which may hinder the accurate quantification of total polyphenol content.[21,22]

In the case of spectrometry-based sensors,[17] disadvantages related to the presence of other non-target interfering compounds can be observed. Conversely, the colorimetric strategy employing benzenediazonium salts appears unaffected by the presence of potential interfering compounds in wine.[16]

Currently, no studies report the use of electromechanical sensors for directly evaluating polyphenols in wine.

Electromechanical sensors are now widely recognized as a robust approach for detecting extremely small masses, while also enabling the assessment of other physical parameters such as film thickness, viscosity, and elasticity.[23] These devices have already demonstrated excellent performance in various research fields such as the detection of clinically relevant proteins,[24] viruses,[25] and bacteria.[.26,27]

Among electromechanical sensors, the Quartz Crystal Microbalance with Dissipation Monitoring (QCM-D) is widely acknowledged as the primary piezoelectric detection method. In this apparatus, the transducer element is typically based on an AT-cut quartz crystal sandwiched between two circular electrodes.[28] When a voltage is applied across the electrodes, the crystal undergoes a deformation in a thickness shear mode. When the frequency of the alternating current (AC) voltage aligns with one of the resonance frequencies of the quartz crystal, which is determined by its thickness and mechanical characteristics, the optimal amplitude of displacement is reached, and an increase in the electric current measured by the electrode is observed.[28,29] As previously stated, through the direct piezoelectric effect, the generated acoustic waves are subsequently converted back into an electric signal, which is then detected at the electrodes.[30–32]

In this system, the adsorption or desorption of molecules from the sensor surface typically causes a change in the resonance frequency. Therefore, monitoring the variations of the resonance frequency enables the collection of information on surface-level phenomena.[28] The coupling of the aforementioned properties with surface functionalization of the quartz crystal surface enables the use of the QCM-D as a biosensoristic technology.

Considerable evidence supports the effectiveness of electromechanical sensors in monitoring polyphenols in oenology. Among them, the QCM-D was reported as an efficient device for wine analysis for different purposes. In the realm of wine safety, the QCM-D has been employed for various critical applications. For instance, it enabled the detection of mycotoxins in wine, such as Ochratoxin A, achieving a Limit of Detection (LOD) of 0.16 ng mL^{-1}.[33]

Additionally, the QCM-D was used to identify in wine the genome of *Brettanomyces bruxellensis*, a yeast that produces harmful chemical compounds and compromises wine quality.[34] Furthermore, the QCM sensor coated with a metal-phenolic film has been applied to detect methanol in alcoholic beverages, a substance known for its detrimental effects on human health.[35]

The QCM-D was applied to better clarify the astringency mechanism in different beverages, such as wine, beer, and tea, demonstrating that the interaction between polyphenols, particularly tannins, and salivary proteins is involved in this sensory perception.[36–38] Other studies[39] provided novel insights about the role of both tartaric acid and pH in the astringency mechanism by QCM-D experiments. The study revealed that within the usual pH ranges (2.3–4.3) and tartaric acid concentrations (0.0–7.0 g L^{-1}) found in wine, the astringency effect is more pronounced at low pH, confirming that this condition mainly impacts the astringency.[39]

Additionally, QCM-D was used to investigate the interaction between specific polyphenols, including (-)-epicatechin (EC), (-)-epigallocatechin (EGC), (-)-epicatechin gallate (ECg), (-)-epigallocatechin gallate (EGCg) and theaflavin-3,3′-digallate, with alpha casein, bovine serum albumin (BSA) and human serum albumin (HAS).[40–43]

Besides, QCM-D provided important insight into the interaction between polyphenols and lipid bilayers. The presence of galloyl units in polyphenols appears to enhance this interac-

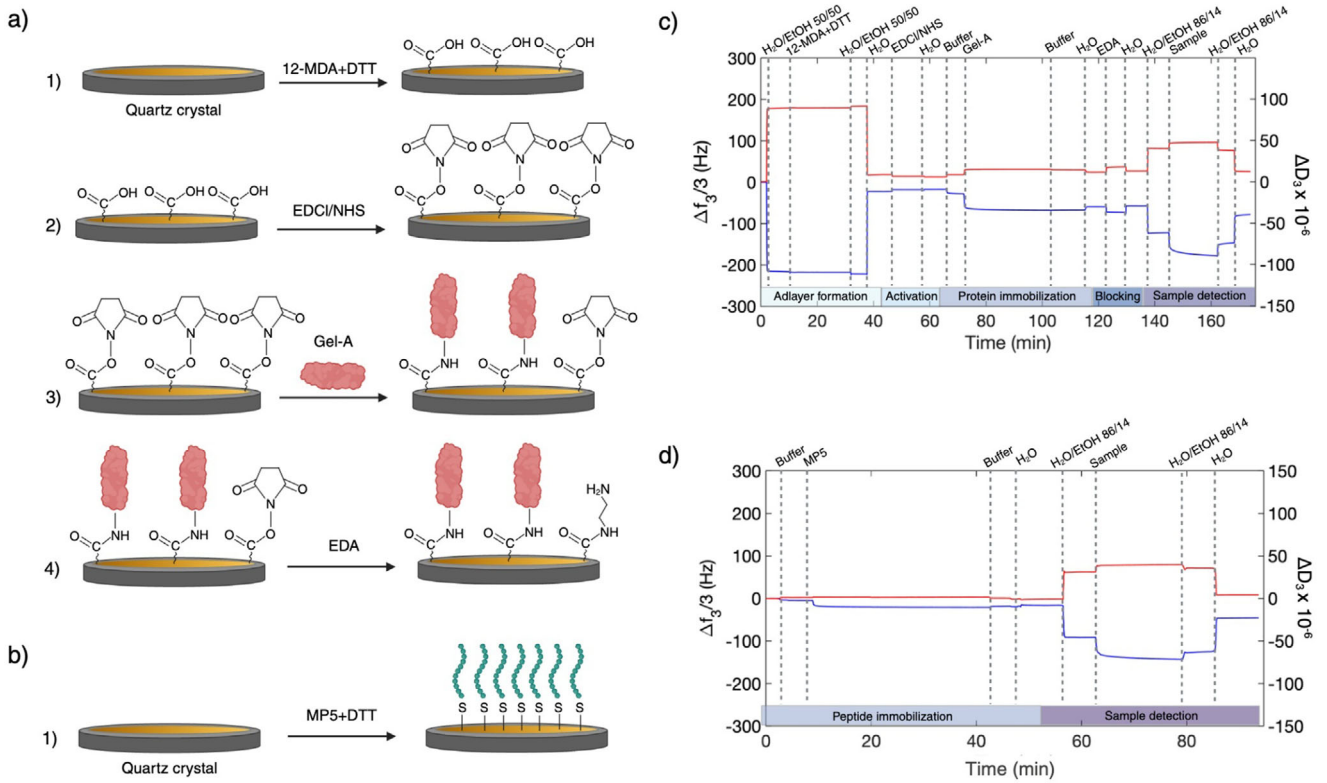

Figure 1. Schematic of the quartz crystal functionalization (not in scale) a) in 1. the formation of the 12-MDA adlayer in presence of DTT as a reducing agent; in 2. the activation of carboxylic acid groups of the adlayer via EDCI/NHS chemistry; in 3. the protein immobilization was achieved through the reaction between the activated adlayer and an aminic group of the selected protein (Gel-A); in 4. deactivation of the residual unreacted NHS-esters with EDA. b) Typical $\Delta f_3/3$ (blue line) and ΔD_3 (red line) traces over time in the case of Gel-A based functionalization (events: Adlayer formation, Activation of carboxylic groups, Protein immobilization, Blocking of residual active esters, and Sample detection). c) the peptide immobilization in the presence of DTT as a reducing agent. d) Typical $\Delta f_3/3$ (blue line) and ΔD_3 (red line) traces over time in the case of MP5-based functionalization (events: Peptide immobilization, Sample detection). Created in BioRender. Tori, G. (2025) https://BioRender.com/o95t497.

tion, as demonstrated by the higher affinity of (-)epicatechin gallate and (-)epigallocatechin gallate to 1,2-dimyristoyl-sn-glycero-3-phospho-choline compared to (-)epicatechin and (-)epigallocatechin.[44]

Finally, another example of the application of electromechanical sensors in the enological field is the use of an Al-based piezoelectric MEMS resonator as a density sensor to monitor the wine fermentation process. In particular, this device has been shown to detect the decrease in sugar concentration and the increase in ethanol concentration.[45]

This study aims to bridge a gap in the literature, as, to our knowledge, there are no reported instances of electromechanical sensors being used for the direct analysis of polyphenols directly in wine. In a previous study, we developed and tested chemical functionalization selected for the analysis of different tannin families in aqueous solutions and in artificial wines, demonstrating their effectiveness.[46] In this study, a subset of these strategies, including Gelatin type A from porcine skin (Gel-A) and of a peptide fragment of Mouse Proline-Rich Protein 5 (MP5), were explored for detecting polyphenols in authentic red wines. Gel-A is commonly used as a wine-fining agent[47] and has been consistently recognized as a reliable probe for polyphenol analysis.[46,48] The selected MP5 fragment represents a single proline-rich repeat of the entire protein, known for its interaction with polyphenols containing galloyl units.[49] As previously demonstrated,[50] this interaction is primarily driven by two forces: the hydrophobic interaction between the pyrrolidine ring of proline and the galloyl ring of polyphenols, and hydrogen bonding, which enhances the stabilization of the complex.

The novelty of this study primarily included the use of optimized surface functionalization protocols for the immobilization of the selected probes.[48] In the case of Gel-A, a protocol that ensured a proper surface coverage to maximize the performance of the sensing system was employed.[48] Furthermore, the study evaluated the probes in the analysis of polyphenols in real wine samples, which are used without any pre-treatment. This posed a significant challenge given the highly complex matrix of red wines, predominantly composed of water, ethanol, alongside glycerol, polysaccharides, organic acids, polyphenols such as anthocyanins and tannins, minerals, and volatile compounds.[51]

2. Results

2.1. Functionalization

The functionalization of the sensors was achieved as shown in **Figure 1**. Regarding Gel-A, the median value of $\Delta f_3/3$ obtained after the adlayer formation (**Table 1**) and probe (**Figure 2**, Table 1)

Table 1. Functionalization results: $\Delta f_3/3$ (Hz), ΔD_3 x 10^{-6}, Molecular density (molecules cm^{-2}) obtained with Gel-A and MP5.

Probe	Step	$\Delta f_3/3$ [Hz]		ΔD_3 x 10^{-6}		Molecular density [molecules cm^{-2}]	
		Median	IQR	Median	IQR	Median	IQR
Gel-A	Adlayer	−23.3	14.9	7.4	6.5	1.1×10^{15}	7.1×10^{14}
	Probe	−36.2	12.0	5.9	1.7	5.1×10^{12}	1.7×10^{12}
MP5	Probe	−12.3	7.9	0.7	1.8	2.1×10^{14}	1.3×10^{14}

immobilization was negative. The median value yielded by MP5 was also negative. Absolute $\Delta f_3/3$ values were higher for Gel-A compared to MP5. The statistical analysis indicated a very highly significant difference between the two distributions (p-value < 0.0001).

The median value of ΔD_3 was higher with Gel-A (5.9×10^{-6}, IQR = 1.7×10^{-6}) compared to MP5 (0.7×10^{-6}, IQR = 1.8×10^{-6}). The statistical analysis revealed a very highly significant difference between the two distributions (p-value< 0.0001).

As described in the Subhead "Data Analysis" of Experimental Section, the molecular density (molecules cm^{-2}) was calculated. Focusing on Gel-A, the median values of the molecular density after adlayer formation and probe immobilization were 1.1×10^{15} and 5.1×10^{12} molecules cm^{-2}, respectively. In the case of MP5, the median of the molecular density was 2.1×10^{14} molecules cm^{-2}. A statistically significant difference was also observed between the molecular density distributions of Gel-A and MP5.

Representative Atomic Force Microscopy (AFM) images of the gold surface before and after functionalization with Gel-A and MP5 are shown in **Figure 3**. The bare gold, measured as a control, revealed an intrinsically rough morphology with a Root Mean Square (RMS) roughness of ≈2.2 nm in the zoomed area. To account for the variability in surface roughness among individual samples, multiple sensors were characterized. The functionalization with MP5 and Gel-A was confirmed by the appearance of a network-like structure on the gold surface, which was also clearly visible in the phase-contrast images. Additionally, the line profiles in Figure 3c–e appeared smoother on the control substrate compared to the functionalized ones. However, the surface roughness seemed to be influenced more by the intrinsic characteristic of the gold surface than by the adsorbed MP5 (RMS ~ 1.4 nm) and Gel-A (RMS ~ 2.2 nm).

The static water contact angle was also measured on the QCM sensors before and after functionalization with Gel-A and MP5, as detailed in (Figure S1, Supporting Information). The characterization revealed a marked increase in surface wettability in the QCM sensor after the completion of the functionalization process.

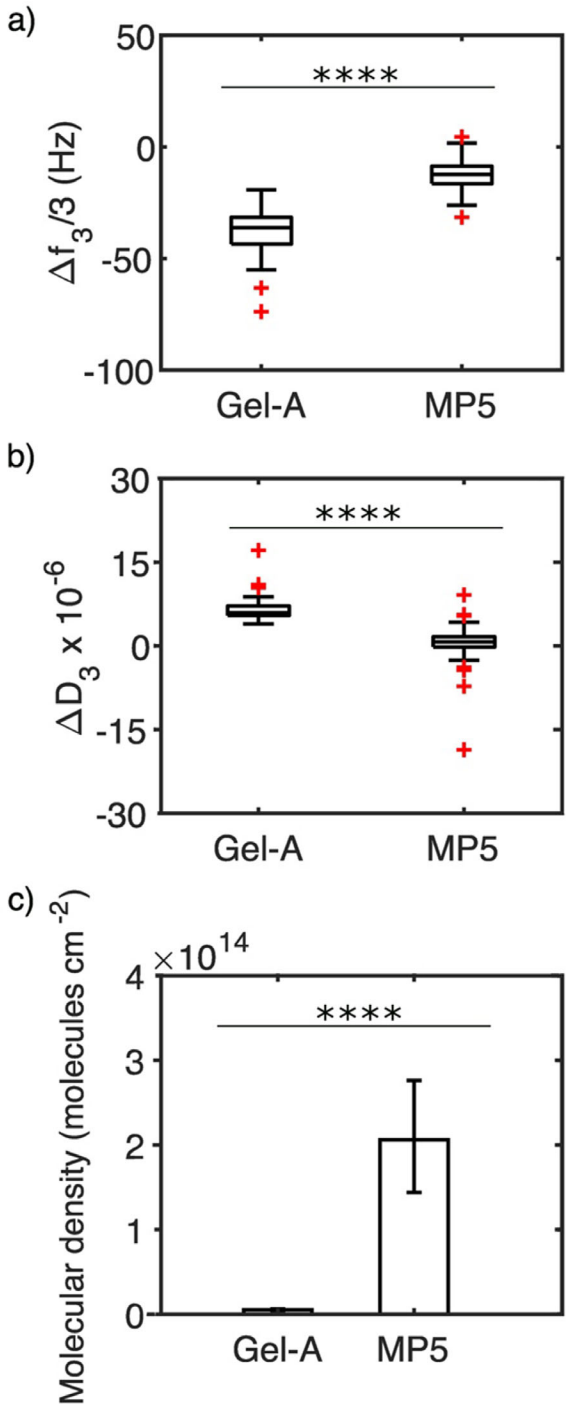

Figure 2. Characterization of the functionalizing layer: a) $\Delta f_3/3$, b) ΔD_3 and c) Molecular density (Molecules cm^{-2}) values after functionalization. The number of experiments for statistical analysis was 46 for Gel-A and 48 for MP5.

2.2. Wine Sample Detection

The effectiveness of Gel-A and MP5 in the analysis of polyphenols was investigated using red wine samples (Table 3). The average $\Delta f_3/3$ and ΔD_3 values (mean ± SE) measured for the wine samples were plotted in **Figure 4**.

When using Gel-A, both negative (Figure 4a,e) and positive (Figure 4c,g) values of $\Delta f_3/3$ were observed. The absolute value of $\Delta f_3/3$ decreased with more diluted samples of L, G, and F wines. On the other hand, B1 displayed a larger $\Delta f_3/3$ compared to B0.

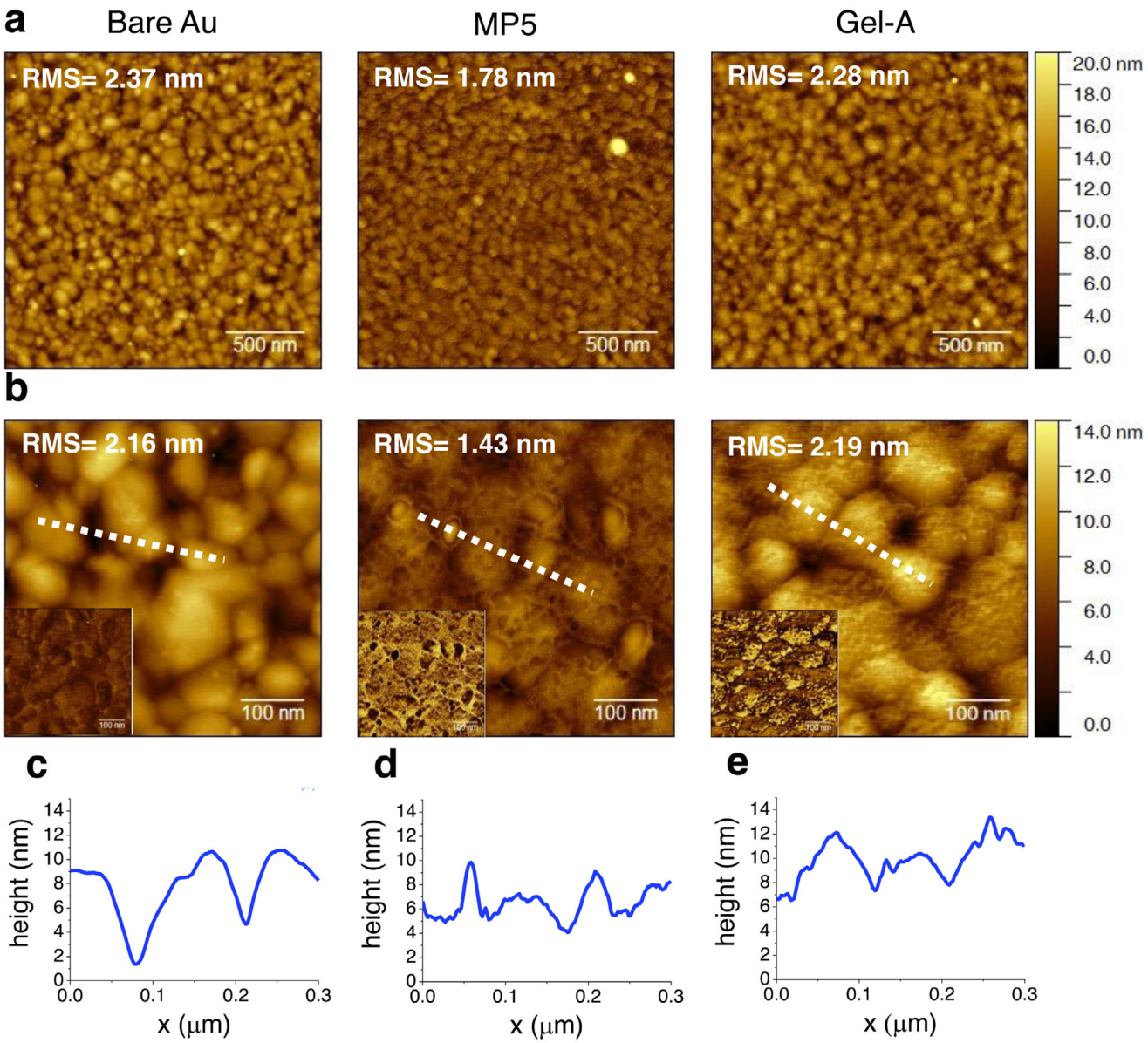

Figure 3. a) AFM topography images of quartz crystal before (Bare Au) and after functionalization with MP5 and Gel-A. b) Higher resolution AFM micrographs of the areas in panel (a). The insets show phase images of the same areas. c–e) AFM height profile, along the dashed lines in the images. The RMS roughness is indicated for each area.

In all instances, ΔD_3 was negative (Figure 4b,d,f,h) and remained relatively consistent across diluted samples in the case of G and B wines, while the dissipation was lower for L1 and F1 compared to the other.

For MP5, negative shifts of $\Delta f_3/3$ were observed for all samples (Figure 4a,c,e,g), due to polyphenols mass loading. A decrease in the absolute value of $\Delta f_3/3$ was noted with G0, G1, G2, and B0, B1, and B2 (Figure 4c,g). The measured $\Delta f_3/3$ was consistent across F0, F1, and F2 (Figure 4e), while L1 exhibited a higher value compared to L0 (Figure 4a). Additionally, ΔD_3 was positive for all samples (Figure 4b,d,f,h).

In the case of MP5, the $\Delta f_3/3$ observed with the sample G0 (Figure 4c), and the ΔD_3 values obtained with L1, L2, and F0 (Figure 4a–f, respectively), were not normally distributed. However, the standard error was plotted for consistency with the other samples in the graphs.

The polyphenolic profiles of the red wines were analyzed using the HPLC technique as reported in Tables S1–S4 (Supporting Information). Subsequently, these data were used to assess the correlation between $\Delta f_3/3$ and ΔD_3 signals and the concentration of different polyphenolic subfamilies. The relationship between $\Delta f_3/3$ and the concentration of total polyphenols was examined for both Gel-A and MP5, as depicted in **Figure 5**. Using Gel-A, no correlation with $\Delta f_3/3$ was observed (Figure 5a), while MP5 showed a decreasing trend with increasing polyphenol concentration (Figure 5c). In contrast, an increasing linear trend was

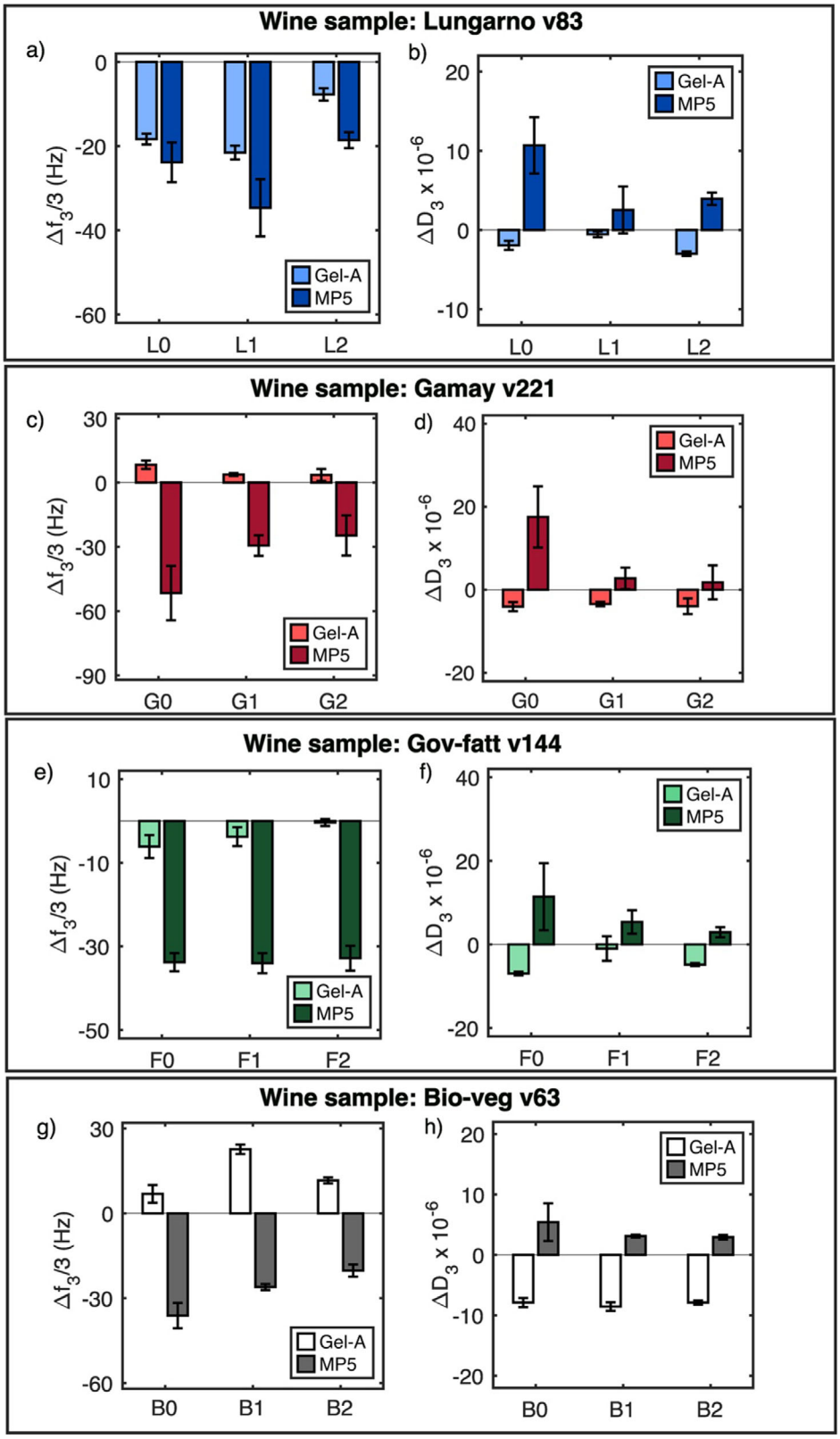

Figure 4. Detection of polyphenols in red wine samples. The frequency ($\Delta f_3/3$) and dissipation (ΔD_3) shifts obtained with the different samples are presented. These values have been grouped to allow a direct comparison of each sample across the two functionalizations. In a, c, e, g) $\Delta f_3/3$ (mean ± SE) values with Gel-A and MP5 obtained with Lungarno, Gamay, Gov-fatt and Bio-Veg wine samples and their corresponding dilutions. In b, d, f, h) ΔD_3 (mean ± SE) values with Gel-A and MP5 obtained with Lungarno, Gamay, Gov-fatt and Bio-Veg wine samples and their corresponding dilutions.

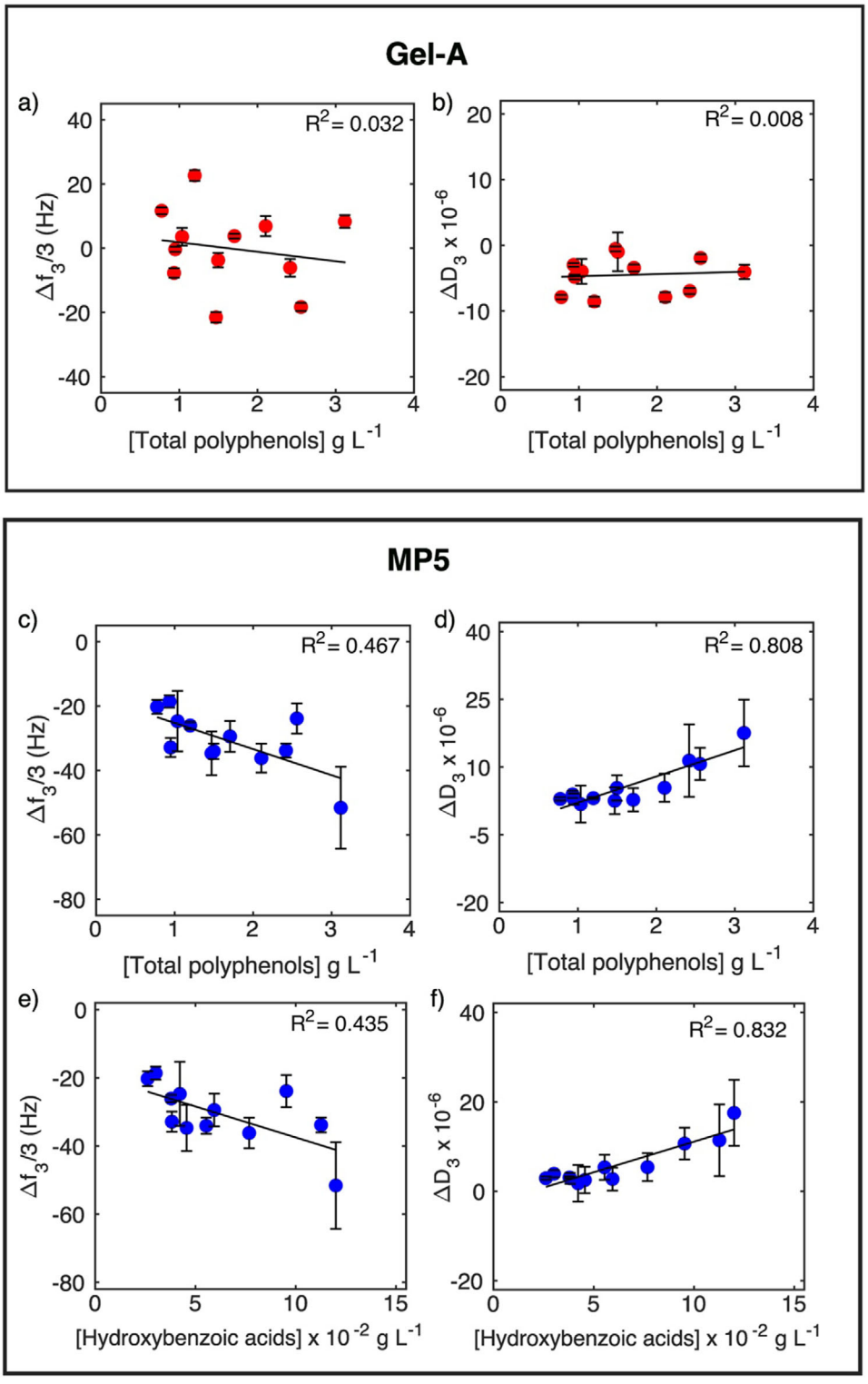

Figure 5. $\Delta f_3/3$ and ΔD_3 values obtained with all wine samples and their respective dilutions, plotted as function of the total polyphenols or hydroxybenzoic acids concentration. In a, b) $\Delta f_3/3$ and ΔD_3 versus total polyphenols concentration using Gel-A. In c, d) $\Delta f_3/3$ and ΔD_3 versus total polyphenols concentration using MP5. In e, f) $\Delta f_3/3$ and ΔD_3 versus hydroxybenzoic acids concentration using MP5.

observed in Figure 5d between ΔD_3 and the concentration of total polyphenols when MP5 was used. Furthermore, a linear trend between ΔD_3 and hydroxybenzoic acid concentration was seen using MP5.

3. Discussion

In this study, the QCM-D was used to investigate the intriguing performance of Gel-A and MP5 in the analysis of polyphenols in red wines.

The functionalization of the QCM-D sensors was correctly accomplished with both Gel-A and MP5, as confirmed by the decrease of the resonance frequency. The $\Delta f_3/3$ values observed using Gel-A were consistent with those observed previously.[48] We observed larger absolute values of $\Delta f_3/3$ with Gel-A compared to MP5. The molecular density (molecules cm^{-2}) was calculated for both Gel-A and MP5 as shown in Subhead "Data Analysis" of Experimental Section using the Sauerbrey model. The use of this model is recommended only for thin and rigid layers, otherwise, the risk is an underestimation of the mass per unit area. Various studies debated its applicability under conditions different from the recommended and established three criteria: i) minimal dependence of $\Delta f_n/n$ on n, ii) ΔD_n values below 2×10^{-6}, and iii) $\Delta D_n/(-\Delta f_n/n) << 4 \times 10^{-7}$ Hz. If any of these criteria are met, the model can be applied. In this study, the second criterion was used to evaluate the Sauerbrey equation's applicability.[52] While the dissipation was very low with MP5, indicating a rigid behavior, the dissipation values obtained with Gel-A were rather higher than 2×10^{-6}. However, contemplating this slight difference, the Sauerbrey model was applied.

The molecular coverage of MP5 was approximately one order of magnitude larger compared to that of Gel-A (the median molecular density was 2.1×10^{14} and 5.1×10^{12} molecules cm^{-2} for MP5 and Gel-A, respectively). The higher molecular density obtained with MP5 might be consistent with the significantly lower molecular weight of MP5 with respect to Gel-A.

The successful chemical modification of the surface is further confirmed by AFM images, which reveal the formation of a network-like structure for both Gel-A and MP5, and by surface wettability measurements, which demonstrate an increased surface hydrophilicity in functionalized QCM sensors.

In detection experiments with MP5, we observed a negative frequency shift with all samples. This behavior was typically related to an increase in the mass adhering to the sensor surface, which we attributed in this scenario to the binding of polyphenols to MP5. In this case, the binding between polyphenols and MP5 is driven by hydrophobic interactions between the aromatic rings of the polyphenols and the proline residues in the peptide. This mechanism has already been demonstrated in Nuclear Magnetic Resonance (NMR) studies,[49] which confirmed that a hydrophobic stacking occurs between the aromatic rings of the polyphenols and the pro-S face of prolines in MP5. Furthermore, these studies highlighted that the first proline within a group of prolines represents the most favored binding site. Additionally, ΔD_3 was positive for all samples, suggesting that the pre-formed layer became more viscoelastic upon interaction with the sample. The dissipation showed a concentration-dependent effect, with diluted samples resulting in lower ΔD_3 values.

Gel-A exhibited both negative and positive frequency shifts, consistent with our previous findings.[46,48] In those studies, positive $\Delta f_3/3$ values were attributed to the formation of non-covalently cross-linked structures between Gel-A and polyphenols.

The interactions between polyphenols and proteins, including gelatin, are well-documented in the literature and can occur through covalent or non-covalent mechanisms. Covalent interactions typically require an alkaline pH and the presence of oxygen. Under these conditions, polyphenols oxidize to quinones, which can undergo nucleophilic attacks by lysine or cysteine residues in the protein chain. In our study, the detection of polyphenols takes place in wine, which has an acidic pH of ≈3 (Table 3). Under such conditions, polyphenols maintain their structural stability, and non-covalent interactions are formed with the protein. These include hydrogen bonding, van der Waals forces, and hydrophobic interactions. Specifically, hydrogen bonds can form between the hydroxyl groups of polyphenols and the carboxylic or aminic groups present in gelatin.[53] Hydrophobic interactions, on the other hand, arise between the aromatic rings of polyphenols and the hydrophobic side chains of gelatin residues. Moreover, such interactions can lead to the development of cross-linked structures between gelatin and polyphenols.[53]

In our interpretation, this also occurred in our system, where upon the formation of such structures, dehydration of the functionalizing layer occurred. Consequently, the observed frequency shift depends both on the increase in mass per unit area due to the adhesion of polyphenols and on the mass per unit area lost due to the dehydration of the functionalization layer. In the case of samples G and B, which exhibit positive frequency shifts, it can be inferred that the mass removed per unit area exceeds that of the bound polyphenols. The dissipation resulted in negative values for all wines, confirming the formation of a network between polyphenols and Gel-A.

HPLC data were used to gain a deeper understanding of this unique behavior of Gel-A. As mentioned above, we supposed that Gel-A developed cross-linked structures with polyphenols, however, we wondered why this effect was particularly pronounced with a subgroup of wine samples. A higher procyanidin content was noted in G and B compared to L and F samples. Procyanidins, also known as condensed tannins, are abundant in phenyl hydroxyl groups[54], which participate in the formation of hydrogen bonds. In literature, the role of procyanidins in the formation of cross-linked structures was well-established.[55] Our hypothesis was that a higher content of procyanidins, which are known to interact with gelatin and act as natural cross-linkers, along with the abundance of hydroxyl groups, crucial for hydrogen bond formation, may explain the different behavior of G and B wines compared to F and L wines

Additionally, Gel-A, which is rich in proline, exhibits an open random coil structure,[56] which was reported to enhance interactions with high molecular weight procyanidins.[56] Furthermore, other studies indicated that Gel-A exhibited an equilibrium binding constant two orders of magnitude higher for grape seeds proanthocyanidins compared to that of tea catechins.[56] In summary, the literature seemed to support our hypothesis, which, however, should be further investigated.

In a biosensor, a linear response of the signal within a specific concentration range of the analyte is desirable, as it facilitates a

Table 2. Overview of sensing approaches for polyphenol detection in wine.

Type of Sensor	Measurement method	Probe layer	Wine pre-treatment	Calibration sample	Detection range	References
Electrochemical	Amperometry	Laccase enzyme from *Trametes versicolor* and *Trametes hirsuta*	Yes	Gallic acid	(0.01-1.70) x 10^{-2} g L^{-1} (0.01-1.80) x 10^{-2} g L^{-1}	[6]
	Amperometry	Laccase enzyme from *Trametes versicolor*	Yes	Caffeic acid	N/A	[7]
	Amperometry	Laccase enzyme from *Coriolus Versicolor*	Yes	Standard equimolar mixtures of catechin and caffeic acid	(0.47-3.29) x 10^{-3} g L^{-1}	[8]
	Amperometry	Laccase enzyme from *Trametes versicolor*	No	Caffeic acid	N/A	[9]
	Amperometry	Laccase enzyme from *Trametes versicolor*	Yes	Gallic acid and caffeic acid	(0.03–8.00) × 10^{-6} g L^{-1} (0.07–10.00) × 10^{-5} g L^{-1}	[10]
	Amperometry	Laccase enzyme from *Trametes versicolor*	Yes	Caffeic acid	(0.90-6.31) × 10^{-3} g L^{-1}	[11]
	Amperometry	Peroxidase enzyme from *Brassica napus*	No	Caffeic acid, t-resveratrol	(0.05-52.00) x 10^{-3} g L^{-1} (0.06-69.00) x 10^{-3} g L^{-1}	[12]
	Amperometry	Tyrosinase from *Mushroom* sp.	Yes	Caffeic acid, phenol, catechol, chlorogenic acid, gallic acid, and protocatechualdehyde	(0.36-36.00) x 10^{-3} g L^{-1} (0.94-37.60) x 10^{-4} g L^{-1} (0.06-55.10) x 10^{-4} g L^{-1} (0.35-70.90) x 10^{-3} g L^{-1} (0.43-15.30) x 10^{-2} g L^{-1} (0.83-82.90) x 10^{-3} g L^{-1}	[13]
	Cyclic voltammetry	N/A	Yes	N/A	N/A	[14]
	Cyclic voltammetry	N/A	Yes	N/A	N/A	[15]
Optical	Colorimetric	Polymer films containing chemically anchored diazonium salts	No	N/A	N/A	[16]
	Spectrophotometry	N/A	No	Tannic acid	(0.51-3.06) x 10^{-1} g L^{-1}	[17]
Electromechanical sensor	Δf, ΔD	Mouse Prolin-Rich Protein 5, Gelatin Type A	No	Wine	0.44-3.59 g L^{-1}	This work

straightforward calibration of the sensors and maintains a constant sensitivity. In the developed biosensor, a linear correlation between the dissipation signal and the total polyphenol concentration was observed in the case of MP5. Additionally, a similar trend was noted between the dissipation shift and the concentration of hydroxybenzoic acids, aligning with the previously reported affinity of proline-rich proteins in saliva for hydrolysable tannins.[57]

In the case of Gel-A, no linear trends were observed. One potential explanation might be that in this case, the $\Delta f_3/3$ was influenced not only by polyphenol mass loading but also by water release resulting from the formation of cross-linked structures. According to this perspective, the presence of both phenomena might explain why the frequency data was not correlated with mass loading.

Table 2 provides a summary of the most common approaches reported in the literature for analyzing polyphenol content in wine. Our electromechanical strategy stands out as competitive compared to existing ones because it offers the advantage of straightforward analysis, enabling direct testing on wine samples without requiring any pre-treatment. Moreover, in contrast to the reported amperometric biosensors, the selected bioreceptors, a peptide and a protein, are more readily available and cost-effective compared to enzymes. Although the proposed strategy is not currently ready for on-site use, it is readily adaptable for this purpose.

Lastly, Table 2 summarizes the detection ranges of various proposed sensors, highlighting the concentration intervals where a linear relationship between total polyphenol concentration and sensor response was observed. In our study, using MP5 as a probe, a linear trend in dissipation was detected in relation to total polyphenol concentrations in wine samples.

Conversely, since in some studies a linear relationship between the sensor response in wine and the total polyphenol concentration was not demonstrated, or such information was not clearly reported, Table 2 provides the linear ranges obtained from sensor calibration using individual polyphenolic compounds as standard analytes.

It is worth noting that, except for our sensor, the detection ranges of the other systems are several orders of magnitude below the total polyphenol concentrations typically found in wine (1–10 g/L). This aspect, along with the ability to measure samples without pre-treatment, the straightforward adaptability of the strategy for on-site analyses, and the low cost of the proposed probes, represents the key strengths of this approach compared to those currently reported in the literature.

Finally, in this study, Gel-A and MP5 were tested with wine samples immediately after the functionalization process. In view

of adapting the proposed system for on-field applications, it will be necessary to conduct dedicated studies to assess the long-term stability of the functionalized sensors and to identify optimal storage conditions to preserve their performance over time. The ultimate goal is to enable sensors to be pre-functionalized and then supplied directly to wineries, allowing them to carry out the measurements without the need for additional preparation steps. This approach would enhance the practicality and user-friendliness of the system in real-world scenarios.

4. Conclusion

The tested probes exhibited noteworthy performance in the analysis of polyphenols in red wines. The primary advantage of our system lies in its high flexibility, which could allow its future adaptation to other electromechanical platforms suitable for on-field measurements. This could provide the desired responses in the winery directly, thus eliminating the need for transportation to specialized laboratories.

An additional development could be the adaptation of the system for the monitoring of wine characteristics over time, for example, during fermentation, aging, and blending.

All the presented findings underscore the potential of the system as a future strategy for assessing both the overall polyphenol content of a wine and the presence of specific polyphenolic subgroups.

The impact of this work could be extended to other areas of the agri-food field, such as the olive oil industry, where polyphenol content influences the flavor of the final product[58] but also its nutritional aspect and storability.

5. Experimental Section

Reagents: Water, hydrogen peroxide solution (30% w/w), ammonium hydroxide solution (28%–30% v/v), sodium dodecyl sulfate (20% in water), phosphate buffer saline (140 mM NaCl, 10 mM phosphate buffer, and 3 mM KCl, pH 7.4 at 25 °C), sodium carbonate (purity degree ≥ 99.5%) and sodium bicarbonate (purity degree ≥ 99.5%) were obtained from Sigma–Aldrich (St. Louis, MO, USA), and ethanol absolute anhydrous and isopropanol were purchased from Carlo Erba Reagents (Milan, Italy).

The functionalization based on the protein involved the use of the following reagents: 12-mercaptododecanoic acid (12-MDA, purity degree 96%, M_w 232.4 Da, Sigma–Aldrich, St. Louis, MO, USA) was used for the formation of the adlayer; 1,4-Dithiothreitol (DTT, $M_{w\ 154.2\ Da,}$ Sigma–Aldrich) for the reduction of 12-MDA molecules; N-(3-Dimethylaminopropyl)-N′-ethylcarbodiimide hydrochloride (EDCl) and N-hydroxyssuccinimide (NHS) for the activation of 12-MDA carboxylic groups (Sigma–Aldrich, purity degree ≥ 98%); Gelatin type A from porcine skin (Gel-A, High bloom, M_w 75.0 kDa, Sigma–Aldrich); ethylene diamine (EDA, Sigma–Aldrich) was employed for the blocking of residual active ester after probe immobilization.

The functionalization based on the peptide required: a fragment of Mouse Proline-Rich Protein 5 (MP5, GPQQRPPQPGNQQGPPPQGGPQC, M_w 2350 Da) with an additional cysteine at the C-terminal end (synthesized by Biomatik Kitchener, Ontario, Canada, purity degree 95%); 1,4-Dithiothreitol (DTT, $M_{w\ 154.2\ Da,}$ Sigma–Aldrich) for the reduction of MP5 molecules.

The wine samples analyzed included: Sensi Lungarno v.83, Sensi Gov-Fatt v144, Sensi Bio-Veg v63, and Sensi Gamay v221 provided by Sensi Vini (Lamporecchio, Italy), as shown in **Table 3**.

Table 3. Wine samples analyzed by QCM-D experiments: sample name, nomenclature, dilution, pH, polyphenol concentration in g L^{-1} of Gallic Acid Equivalent, measured via the Folin–Ciocalteu method; each value represents mean ± standard deviation ($n = 3$).

Sample Name	Nomenclature	Dilution	pH	Polyphenol Concentration [g L^{-1}]
Sensi Lugarno V83	L0	1:0	3.56	2.453 ± 0.047
	L1	1:1	3.44	1.241 ± 0.041
	L2	1:2	3.38	0.637 ± 0.019
Sensi Gov-Fatt V144	F0	0	3.58	1.999 ± 0.021
	F1	1:1	3.44	0.999 ± 0.032
	F2	1:2	3.37	0.509 ± 0.005
Sensi Bio-Veg V63	B0	0	3.57	1.444 ± 0.029
	B1	1:1	3.45	0.788 ± 0.037
	B2	1:2	3.37	0.437 ± 0.006
Sensi Gamay V221	G0	0	3.53	3.587 ± 0.003
	G1	1:1	3.42	1.825 ± 0.030
	G2	1:2	3.36	0.927 ± 0.004

Quartz Crystal Microbalance with Dissipation Monitoring (QCM-D) Experiments: The QCM-D (E4 model, Q-Sense AB, Sweden) experiments were carried out using AT-cut quartz crystals, with a fundamental resonance frequency of 5 MHz (diameter = 14 mm, Biolin Scientific, Västra Frölunda, Sweden). The quartz crystals used in QCM-D experiments underwent a six-step cleaning process: i) rinsing with 2% sodium dodecyl sulfate, ii) treatment with oxygen plasma (Femto Diener, Diener electronic GmbH & Co., Ebhausen, Germany) for 2 min at a power of 100 W, iii) chemical treatment with a 5:1:1 solution of water, ammonia, and hydrogen peroxide for 15 min, iv) rinsing with water, v) rinsing with isopropanol, vi) treatment with oxygen plasma under the same conditions (2 min, 100 W).

The measurements were accomplished in temperature-controlled conditions (25 °C). QCM-D measurements involved monitoring changes in both resonance frequency (Δf) and energy dissipation (ΔD), focusing on odd overtone from the 1st to the 13th, by exciting the fundamental resonance frequency of the quartz crystal. Among the 7 overtones, the 3rd was selected as it showed more reliable performance throughout the acquisitions.

Sensor Functionalization: The functionalization of the sensor surface was achieved by exploiting the thiol-gold chemistry. Since Gel-A lacks free thiol groups, the functionalization was accomplished in a three-step process. The surface was previously modified using a linker, 12-MDA, with its thiol groups used for the immobilization. Subsequently, the carboxylic groups of 12-MDA were activated using EDCl/NHS chemistry, and then the protein was immobilized. The linker solution was prepared by combining 12-MDA and DTT (0.1x mol/mol with respect to free -SH groups) in a 50% v/v water/ethanol mixture (12-MDA concentration 2 mg mL^{-1}). For all the solutions mentioned hereafter, 500 µL were injected. This volume was chosen to fully fill the chamber containing the sensor. Before the injection of the linker solution, the QCM-D apparatus was conditioned in a 50% v/v water/ethanol mixture, then the linker solution was injected and incubated for 30 min. Then, the sensor was rinsed with a 50% water/ethanol solution (5 min) and with water (5 min). This produced a self-assembled monolayer (SAM) of 12-MDA with carboxylic groups available for the subsequent protein immobilization. Afterward, a water solution of EDCl/NHS (10 mM each) was injected and incubated for 15 min to activate the carboxylic functionalities. The sensor was rinsed with water for 5 min.

At this stage, the protein conjugation was performed at pH 9 using a carbonate/bicarbonate buffer. The protein immobilization was performed at pH 9, close to the isoelectric point of Gel-A. This ensured that the Gel-A molecules predominantly exhibited a neutral net charge, minimizing repul-

sion among them. The apparatus was initially conditioned with the buffer for 5 min, and then the protein solution was injected (1 mg mL^{-1}) for 30 min. The protein solution was rinsed with the same buffer for 5 min and with water for 5 min.

Finally, residual NHS-esters were deactivated by injecting a 0.1 M EDA solution in water for 5 min, followed by water rinsing (5 min). A representation of the functionalization steps for the protein is outlined in Figure 1a, with a corresponding typical trace of $\Delta f_3/3$ and ΔD_3 over time in Figure 1b.

In the case of MP5, the functionalization of the sensor surface was obtained in a single step, due to the cysteine at the C-terminal end of the peptide, as shown in Figure 1c. The apparatus was initially conditioned in PBS 1x buffer for 5 min, then MP5 solution in PBS 1x (1 mg mL^{-1}) supplemented with DTT (3.5x mol/mol with respect to free -SH) was injected and incubated for 30 min. Finally, the sensor was rinsed with PBS 1x (5 min) and with water (5 min). In Figure 1d a typical trace of $\Delta f_3/3$ and ΔD_3 trace over time is shown.

AFM Characterization: Atomic force microscopy (Dimension Icon, Bruker, Billerica, MA, USA) operating in Soft Tapping mode was used to assess the morphology and to estimate the roughness of the sensor surface before and after the completion functionalization process for both the tested probes. Samples were measured at room temperature and pressure, under an air atmosphere. Data were elaborated using Gwyddion software (Gwyddion version 2.54, Brno, Czech Republic, available at http://gwyddion.net/).

Wine Samples Detection Experiments: Total polyphenol concentration of the wine samples was measured via the Folin–Ciocalteu method. The wine samples analyzed (Table 3) were stored at 4 °C before use. Once the functionalization was completed, 500 µL of a water/ethanol blend containing 14% of ethanol was injected the signal was stabilized in a 14% water/ethanol blend (v/v) (5 min). This percentage was chosen to reflect the average alcohol content of the analyzed wines, which was between 12.6 and 14.7 (water/ethanol v/v). Then, the wine samples were injected and incubated for 15 min. Finally, the sensor was rinsed with a 14% water-ethanol blend (v/v) (5 min) and with water (5 min). All the steps in the sample detection stage are shown in Figure 1b,d (respectively for Gel-A and MP5.

Data Analysis: Throughout the QCM-D experiments, $\Delta f_n/n$ and ΔD_n were continuously monitored. Despite QCM-D capability to record multiple harmonics of frequency and dissipation, our analysis was mainly focused on the third harmonic (Δf_3, ΔD_3) due to its enhanced stability. The utilization of a single harmonic did not affect the final interpretation of the data.

A total of 94 independent sensors were used for the presented experiments. Of these, 46 sensors were functionalized with Gel-A and 48 with MP5. The sensors were functionalized on different days, using different stock solutions, and in separate chambers of the instrument. Subsequently, both the sensors functionalized with Gel-A and those with MP5 were employed to analyze 12 distinct wine samples. Each wine was analyzed at least three times using different sensors with both functionalizations.

The QCM-D raw data were analyzed using a MATLAB in house-script (MATLAB version R2022b, Mathworks, Natick, MA, USA). During each phase of the experiment, a baseline in water was recorded for ≈5 min before the injection of any solution. The reported $\Delta f_3/3$ and ΔD_3 values were derived by computing the difference between the initial baseline in water and the readings obtained after the water rinse.

The number of molecules per cm^2 was determined as follows. The areal mass Δm (ng cm^{-2}), which represents the mass adhered per unit area of the sensor, was derived using the Sauerbrey equation[52]:

$$\Delta m = -C\,\Delta f_n/n \tag{1}$$

The subscript n indicates the overtone number. The constant C is called the mass sensitivity constant, and it is equal to 17.7 ng cm^{-2} Hz^{-1} for a 5 MHz quartz crystal. Δf_n refers to the frequency shift of a specific overtone.

Then the molecular density (molecules cm^{-2}) was calculated as follows:

$$\text{molecular density} = \frac{\Delta m}{Mw} \cdot NA \tag{2}$$

In Equation (2) Mw (g mol^{-1}) represents the molecular weight of the immobilized molecule, and NA is the Avogadro number (6.022×10^{23} mol^{-1}). For the calculation of the molecular density after the adlayer formation, an average molecular weight of 225.35 Da was used, because we accounted for the presence of DTT 0.1x alongside 12-MDA in the linker solution.

For the calculation of the molecular density after MP5 immobilization, an average molecular weight of 637.32 Da was used, considering the presence of DTT 3.5x in the peptide immobilization solution.

The $\Delta f_3/3$, ΔD_3 values obtained after the functionalization process were displayed in box plots, considering the values falling outside 1.5 times the interquartile range (IQR) from the box as outliers. The calculated molecular density was displayed in bar plots where the height of the bar represented the median, while the error bars corresponded to the IQR. The statistical analysis was performed using MATLAB Statistics and Machine Learning Toolbox (v 23.2, Mathworks, Natick, MA, USA). The normality of these distributions was assessed using the Shapiro-Wilk test,[59] and $\Delta f_3/3$, ΔD_3, and molecular coverage obtained with Gel-A and MP5 at the end of the functionalization were compared using the Wilcoxon rank-sum test.[60] The significance threshold was set to 0.05.

The Δf_3, ΔD_3 values obtained with the different wine samples were displayed in a bar plot, where the height of the bar represented the mean of at least three replicates, and the corresponding error bars represented the standard error.

Additionally, correlations between $\Delta f_3/3$, ΔD_3 obtained with Gel-A and MP5, and the concentrations of total polyphenols or specific polyphenol subgroups were analyzed. These correlations were depicted in scatter plots, showing $\Delta f_3/3$ or ΔD_3 versus analyte concentration. Linear trends were evaluated using the MATLAB fitlm function, which also provided the coefficient of determination (R^2) for the fits.[60]

Declaration of Generative AI and AI-Assisted Technologies in the Writing Process: During the preparation of this work, the authors used ChatGPT in the drafting process in order to enhance the clarity and language of the manuscript. After using this tool, the authors reviewed and edited the content as needed and take full responsibility for the content of the published article.

Supporting Information

Supporting Information is available from the Wiley Online Library or from the author.

Acknowledgements

This research was funded by the Italian Ministry of University and Research (MUR) with the project "VioLOC – Wine and Oil Analysis 4.0: development of a Lab-On-Chip with remote connectivity," FISR 2019, Grant FISR2019-03020. The authors thank Sensi Vigne & Vini S.r.l. for having provided wine samples.

Conflict of Interest

The authors declare no conflict of interest.

Data Availability Statement

Complete datasets are available on the ZENODO platform (link: zenodo.org/records/13133183).[61]

Keywords

biosensor, polyphenols, precision oenology, QCM, Quartz Crystal Microbalance

Received: December 13, 2024
Revised: March 27, 2025
Published online: June 6, 2025

[1] M. Daglia, *Curr. Opin. Biotechnol.* **2012**, *23*, 174.
[2] R. Gutiérrez-Escobar, M. J. Aliaño-González, E. Cantos-Villar, *Molecules* **2021**, *26*, 718.
[3] V. C. Niculescu, N. Paun, R. E. Ionete, in *Grapes and Wines-Advances in Production, Processing, Analysis and Valorization*, *7*, Intech Open, London, UK **2018**, 119.
[4] B. Lorrain, I. Ky, L. Pechamat, P. L. Teissedre, *Molecules* **2013**, *18*, 1076.
[5] M. C. Vlasiou, *Dairy*, **2023**, *4*, 509.
[6] M. Di Fusco, C. Tortolini, D. Deriu, F. Mazzei, *Talanta* **2010**, *81*, 235.
[7] C. I. S. Fernandes, M. J. F. Rebelo, *Portugaliae Electrochim. Acta* **2009**, *27*, 457.
[8] S. A. S. S. Gomes, J. M. F. Nogueira, M. J. F. Rebelo, *Biosens. Bioelectron.* **2004**, *20*, 1211.
[9] D. M. Gil, M. J. Rebelo, *Eur. Food Res. Technol.* **2010**, *231*, 303.
[10] M. Gamella, S. Campuzano, A. J. Reviejo, J. M. Pingarrón, *J. Agric. Food Chem.* **2006**, *54*, 7960.
[11] A. R. S. Júnior, M. J. F. Rebelo, *Portugaliae Electrochim. Acta* **2008**, *26*, 117.
[12] A. M. Granero, H. Fernández, E. Agostini, M. A. Zón, *Talanta* **2010**, *83*, 249.
[13] V. C. Sanz, M. L. Mena, A. González-Cortés, P. Yanez-Sedeno, J. M. Pingarrón, *Anal. Chim. Acta* **2005**, *528*.
[14] P. A. Kilmartin, *Antioxid. Redox Signal.* **2001**, *3*, 941.
[15] P. A. Kilmartin, H. Zou, A. L. Waterhouse, *J. Agric. Food Chem.* **2001**, *49*, 1957.
[16] S. Vallejos Calzada, D. Moreno Mediavilla, S. I. Cortes, M. A. Muñoz Santamaría, F. C. García García, J. M. García Pérez, *Food Control* **2019**, *106*, 106684.
[17] S. V. Oscar, O. C. L. Fernando, C. M. M. Del Pilar, *Food Chem.* **2017**, *221*, 1062.
[18] R. Fopase, S. Paramasivam, P. Kale, B. Paramasivan, *J. Environ. Chem. Eng.* **2020**, *8*, 104266.
[19] G. Sun, X. Wei, D. Zhang, L. Huang, H. Liu, H. Fang, *Biosensors* **2023**, *13*, 886.
[20] Dhanjai, X. L.u, L. Wu, J. Chen, Y. Lu, *Anal. Chem.* **2020**, *92*, 5830.
[21] Â. Vilas-Boas, P. Valderrama, N. Fontes, D. Geraldo, F. Bento, *Food Chem.* **2019**, *276*, 719.
[22] R. C. Martins, R. Oliveira, F. Bento, D. Geraldo, V. V. Lopes, P. Guedes de Pinho, A. C. Silva Ferreira, *J. Agric. Food Chem.* **2008**, *56*, 12092.
[23] M. V. Voinova, *J. Sensors* **2009**, *2009*, 943125.
[24] M. Agostini, F. Amato, M. L. Vieri, G. Greco, I. Tonazzini, L. Baroncelli, M. Caleo, E. Vannini, M. Santi, G. Signore, M. Cecchini, *Biosens. Bioelectron.* **2021**, *172*, 112774.
[25] M. Agostini, F. Lunardelli, M. Gagliardi, A. Miranda, L. Lamanna, A. G. Luminare, F. Gambineri, M. Lai, M. Pistello, M. Cecchini, *Adv. Funct. Mater.* **2021**, *32*, 2201958.
[26] M. Gagliardi, M. Agostini, F. Lunardelli, L. Lamanna, A. Miranda, A. Bazzichi, A. G. Luminare, F. Cervelli, F. Gambineri, M. Totaro, M. Lai, G. Maisetta, Batoni, M. P., M. Cecchini, *Sens. Actuators, B* **2023**, *379*, 133299.
[27] Y. W. Kim, S. E. Sardari, M. T. Meyer, A. A. Iliadis, H. C. Wu, W. E. Bentley, R. Ghodssi, *Sens. Actuators, B* **2012**, *163*, 136.
[28] R. Fogel, J. Limson, A. Seshia, *Essays in Biochemistry* **2016**, *60*, 101.
[29] D. Johannsmann, in *Soft and Biological Matter*, Springer, Cham, **2015**.
[30] A. A. M. Ralib, A. N. Nordin, *IIUM Eng. J.* **2024**, *15*, https://doi.org/10.31436/iiumej.v15i2.437.
[31] D. W. Grainger, D. G. Castner, in *Comprehensive Biomaterials II*, Elsevier, Amsterdam, The Netherlands **2017**, pp. 1–24.
[32] N. L. L. Hekiem, A. A. M. Ralib, F. B. Ahmad, A. N. Nordin, R. Ab Rahim, N. F. Za'bah, *Sens. Actuators, A* **2021**, *329*, 112792.
[33] A. Karczmarczyk, K. Haupt, K. H. Feller, *Talanta* **2017**, *166*, 193.
[34] S. Poggesi, L. Zhou, G. C. Bariani, R. Mittapalli, M. Manzano, R. E. Ionescu, *Crystals* **2021**, *11*, 562.
[35] K. D. Esmeryan, Y. Lazarov, T. Grakov, Y. I. Fedchenko, L. G. Vergov, S. Staykov, *Micromachines* **2023**, *14*, 1274.
[36] Y. Yan, J. Hu, P. Yao, *Langmuir* **2009**, *25*, 397.
[37] H. Kaneda, J. Watari, M. Takashio, Y. Okahata, *J. Am. Soc. Brew. Chem.* **2004**, *61*, 119.
[38] S. Wang, S. M. Olarte Mantilla, P. A. Smith, J. R. Stokes, H. E. Smyth, *Food Hydrocolloids* **2021**, *120*, 106918.
[39] Q. Zhao, G. Du, S. Wang, P. Zhao, X. Cao, C. Cheng, H. Liu, Y. Xue, X. Wang, *Food Chem.* **2023**, *403*, 134385.
[40] X. Wang, C. T. Ho, Q. Huang, *J. Agric. Food Chem.* **2007**, *55*, 4987.
[41] M. Weerawatanakorn, Q. Huang, C. T. Ho, *Int. Food Res. J.* **2014**, *21*, 493.
[42] E. E. Ali, M. O. Elmakki, M. L. Gavette, B. J. Doyle, S. J. Timpe, *Biochem. Res. Int.* **2019**, *2019*, 6154170.
[43] K. Minoda, T. Ichikawa, T. Katsumata, K. I. Onobori, T. Mori, Y. Suzuki, T. Ishii, T. Nakayama, *J. Nutr. Sci. Vitaminol.* **2010**, *56*, 331.
[44] M. Kamihira, H. Nakazawa, A. Kira, Y. Mizutani, M. Nakamura, T. Nakayama, *Biosci., Biotechnol. Biochem.* **2008**, *72*, 1372.
[45] J. Toledo, V. Ruiz-Díez, G. Pfusterschmied, U. Schmid, J. L. Sánchez-Rojas, *Sens. Actuators, B* **2018**, *254*, 291.
[46] M. Gagliardi, G. Tori, M. Agostini, F. Lunardelli, F. Mencarelli, C. Sanmartin, M. Cecchini, *Nanomaterials* **2022**, *12*, 166.
[47] F. Cosme, J. M. Ricardo-Da-Silva, O. Laureano, *Italian J. Food Sci.* **2007**, *19*, 39.
[48] M. Gagliardi, G. Tori, C. Sanmartin, M. Cecchini, *J. Sci. Food Agric.* **2024**, *105*, 1476.
[49] N. J. Baxter, T. H. Lilley, E. Haslam, M. P. Williamson, *Biochemistry* **1997**, *36*, 5566.
[50] N. J. Murray, M. P. Williamson, T. H. Lilley, E. Haslam, *Eur. J. Biochem.* **1994**, *219*, 923.
[51] B. Nemzer, D. Kalita, A. Y. Yashin, Y. I. Yashin, *Beverages* **2022**, *8*, 1.
[52] A. Saftics, S. Kurunczi, B. Peter, I. Szekacs, J. J. Ramsden, R. Horvath, *Adv. Colloid Interface Sci.* **2021**, *294*, 102431.
[53] N. Cao, Y. Fu, J. He, *Food Hydrocolloids* **2007**, *21*, 575.
[54] H. Yang, X. Tuo, L. Wang, R. Tundis, M. P. Portillo, J. Simal-Gandara, Y. Yu, L. Zou, J. Xiao, J. Deng, *Trends Food Sci. Technol.* **2021**, *111*, 114.
[55] L. He, C. Mu, J. Shi, Q. Zhang, B. Shi, W. Lin, *Int. J. Biol. Macromol.* **2011**, *48*, 354.
[56] R. A. Frazier, E. R. Deaville, R. J. Green, E. Stringano, I. Willoughby, J. Plant, I. Mueller-Harvey, *J. Pharm. Biomed. Anal.* **2010**, *51*, 490.
[57] J. R. Bacon, M. J. C. Rhodes, *J. Agric. Food Chem.* **2000**, *48*, 838.
[58] F. Angerosa, R. Mostallino, C. Basti, R. Vito, *Food Chem.* **2000**, *68*, 283.
[59] A. BenSaïda, Shapiro-Wilk and Shapiro-Francia normality tests https://www.mathworks.com/matlabcentral/fileexchange/13964-shapiro-wilk-and-shapirofrancia-normality-tests, (accessed: April 2024).
[60] The MathWorks Inc., in *Statistics and Machine Learning Toolbox Documentation*, The MathWorks Inc., Natick, MA, USA **2021**.
[61] G. Tori, M. Gagliardi, F. Lunardelli, C. Sanmartin, I. Taglieri, G. Alfieri, M. Modesti, A. Bellincontro, F. Mencarelli, M. Cecchini, *Zenodo*, **2024**, https://doi.org/10.5281/zenodo.13133182.